

Multiple-Quantum Transitions and Charge-Induced Decoherence of Donor Nuclear Spins in Silicon

David P. Franke,^{1,*} Moritz P. D. Pflüger,¹ Kohei M. Itoh,² and Martin S. Brandt¹

¹Walter Schottky Institut and Physik-Department, Technische Universität München, Am Coulombwall 4, 85748 Garching, Germany

²School of Fundamental Science and Technology, Keio University, 3-14-1 Hiyoshi, Kohoku-ku, Yokohama 223-8522, Japan

(Received 13 October 2016; revised manuscript received 13 January 2017; published 15 June 2017)

We study single- and multi-quantum transitions of the nuclear spins of an ensemble of ionized arsenic donors in silicon and find quadrupolar effects on the coherence times, which we link to fluctuating electrical field gradients present after the application of light and bias voltage pulses. To determine the coherence times of superpositions of all orders in the 4-dimensional Hilbert space, we use a phase-cycling technique and find that, when electrical effects were allowed to decay, these times scale as expected for a fieldlike decoherence mechanism such as the interaction with surrounding ²⁹Si nuclear spins.

DOI: 10.1103/PhysRevLett.118.246401

Aiming for the realization of a scalable quantum technology, the electron and nuclear spins of phosphorus donors in silicon have been studied extensively [1–8]. Because of different interaction strengths with their surroundings, they form a powerful combination of a fast, but more volatile electron spin and a slower, but very coherent nuclear spin qubit [9–11]. This nuclear spin is $I = 1/2$ for phosphorus, but systems with a higher nuclear spin can be realized by simply replacing phosphorus by the other hydrogenic donors As ($I = 3/2$) [12,13], Sb ($5/2$ and $7/2$) [14,15], and Bi ($9/2$) [16–18]. Several advantages of the d -dimensional Hilbert spaces of such systems, sometimes called qudits, have been proposed, such as the realization of simpler and more efficient gates [19,20] or more secure quantum cryptography [21]. In addition, one higher order system can replace several qubits, simplifying their physical implementation [22]. These concepts usually require coherent superpositions of higher orders, which show specific interactions with their surroundings that can be reflected in the observed coherence times. In particular, the additional quadrupole interaction with electric field gradients arising from strain [13,23,24] or defect states [25] has to be considered for heavier dopants. In this work, we study first- and higher-order coherences of ionized As donors in silicon. By including light and voltage pulses in the experiment, we are able to link the additional quadrupolar decoherence effect observed in our previous work [13] to the electrical environment of the nucleus and show that it vanishes, when charges in the sample are allowed to relax. In addition, we use a phase-cycling technique to study superpositions of all orders and find that the coherence times scale inversely proportional to the coherence order, as expected for a fieldlike decoherence mechanism such as the interaction with surrounding ²⁹Si nuclear spins.

The Hamiltonian \mathcal{H} characterizing ionized arsenic donors with nuclear spin $\mathbf{I} = \{I_x, I_y, I_z\}$ in a magnetic field B_z can be written as

$$\mathcal{H}/h = -\nu_0 I_z + \nu_Q \frac{1}{2} \left(I_z^2 - \frac{5}{4} \right), \quad (1)$$

where $\nu_0 = \gamma_n B_z$ with the nuclear gyromagnetic ratio γ_n and h is Planck's constant. The second term on the right-hand side of (1) describes the nuclear quadrupole interaction with an effective electric field gradient. In the samples studied here [13], we can assume this gradient to be uniaxial and hence fully described by the main component V_{33} in its principle axes system [26]. In first order approximation, ν_Q is then given by

$$h\nu_Q = \frac{1}{2} V_{33} eQ \frac{1}{2} (3\cos^2\vartheta - 1), \quad (2)$$

where Q is the nuclear quadrupole moment, e is the elementary charge, and ϑ describes the angle between B_z and V_{33} . The effect of this interaction on the eigenstates of \mathcal{H} is depicted in Fig. 1(a). For hydrogenic donors in silicon, the quadrupole interaction usually vanishes because of the cubic symmetry of the crystal. Then, the spin states are determined by the nuclear Zeeman interaction only, which leads to four equally spaced levels with transition frequencies ν_0 . However, if a strain ϵ is applied to the sample and this symmetry is broken, $\nu_Q \neq 0$ and the eigenenergies are shifted [13].

The coherent superpositions, or coherences, in the four-dimensional Hilbert space can be classified by their coherence order $p = m_I^{(i)} - m_I^{(j)}$, where $m_I^{(i)}$ and $m_I^{(j)}$ are the nuclear spin projections of the superimposed states. Following nuclear magnetic resonance (NMR) literature, we will call coherences of order $|p| = 1, 2,$ and 3 single-, double-, and triple-quantum transitions (SQTs, DQTs, and TQTs), respectively [27]. To characterize them, we will follow two different approaches: First, we will study the SQTs in a strained Si sample, where ν_Q is large compared to the linewidth of the resonance signal [13]. In this case,

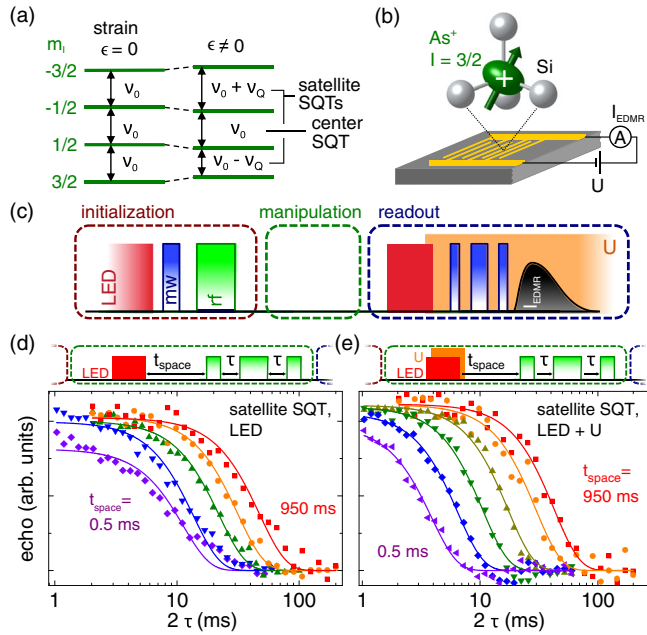


FIG. 1. (a) Energy levels of the nuclear spin of ionized donors As^+ in Si with and without an electric field gradient caused by a strain ϵ . (b) Schematic representation of the sample and the interdigit contact structure. (c) Schematic representation of the ENDOR pulse sequence used in this work. Examples for manipulation pulse sequence are given on top of (d) and (e). Echo decays of a satellite SQT (d) for a 500- μ s-long light pulse and $t_{space} = 0.5, 2.5, 20, 80,$ and 950 ms and (e) for a 500- μ s-long combined light and bias voltage pulse and $t_{space} = 0.5, 2.5, 10, 80, 300,$ and 950 ms. Solid lines represent fits with superexponential decays ($\alpha = 2$).

the resonances corresponding to the three SQTs do not overlap [13] and T_2 for the satellite and center SQTs can easily be measured separately, allowing us to single out the effect of ν_Q . Second, we will measure coherences of all orders in a sample without strain. While, due to selection rules, generally only transitions with $\Delta m_I = \pm 1$ can be addressed directly in NMR experiments, higher order coherences can be created by driving degenerate transitions with nonselective pulses, as will be discussed below.

The experiments were performed on [111]- and [110]-oriented Si samples that were implanted with As^+ ions (depth ~ 50 – 80 nm) and not annealed, conserving the implantation defects. This provides an efficient pair recombination process for electrically detected magnetic resonance (EDMR) [28–30]; from the magnitude of the EDMR signal we estimate the number of As donors observed to be of the order of 10^6 . The [111]-oriented sample was thinned and cemented to a sapphire substrate, which at low temperatures generates a compressive strain due to the different thermal extension coefficients of the materials [13]. Nuclear spin transitions and echoes are measured by electrically detected electron nuclear double resonance (ENDOR) which is described in detail in

Refs. [13,31,32] and will be reviewed briefly below. The experiments were performed in a Bruker flexline resonator for pulsed ENDOR in a He-flow cryostat at 8 K, the microwave frequency was 9.74 GHz, and illumination was provided by a red light-emitting diode. The bias voltage U of typically 8 V was applied via an interdigit contact structure with a separation of 10 μ m [Fig. 1(b)] and pulsed using an optoisolator.

The basic light, microwave (mw), and radio frequency (rf) pulse sequence used in this study is shown schematically in Fig. 1(c). Combining selective mw pulses and rf pulses, a high nuclear spin polarization is achieved (initialization) [31,32]. After relaxation to the ionized charge state, additional rf pulses, such as an echo sequence, can be applied (manipulation) [13]. At the end of the sequence, the sample is illuminated to transfer the donors to the neutral charge state and detect the nuclear spin state via application of an electron spin echo and evaluation of the current transient I_{EDMR} after the last mw pulse (readout).

We first study the coherence times T_2 of the satellite and center SQTs (sSQT and cSQT, respectively) on the strained sample, where the two transitions can easily be separated. In our previous work [13], we have found T_2^{sSQT} of the sSQTs to be significantly shorter than T_2^{cSQT} of the cSQT. This was attributed to the influence of the quadrupole interaction, and in particular to interactions with lattice vibrations (phonons) or local charges. While the former can be excluded from a missing temperature dependence, trapping and later recombination of charges, e.g. at implantation defects, could lead to changes in the field gradients which would in turn decohere the nuclear spin. To analyze the influence of such effects, we systematically change the electronic environment of the ionized donors in our experiment by introducing either a light pulse (LED) or a combined light-voltage pulse (LED + U) in the sequence. These pulses are inserted 5 ms after the initialization and a variable time t_{space} is added before the nuclear spin echo rf sequence. The resulting sSQT echo decay traces for light and light-voltage pulses are shown in Figs. 1(d) and 1(e), respectively. A strong influence of t_{space} on the decay is observed in both experimental series. The decays can be fitted by superexponential functions $\exp(-2\tau/T_2)^\alpha$ with $\alpha = 2$, and the extracted coherence times T_2 are plotted as a function of t_{space} in Fig. 2(a). Clearly, the coherence time rises systematically with longer t_{space} , and seems to approach saturation at $T_2 \approx 50$ ms for $t_{space} > 1$ s, where the experiment was discontinued because of the long measuring times involved. However, the values at 1 s are within error equal for both measurement series and also equal to the T_2 of the cSQT, which is not influenced by the implementation of the additional pulses (data not shown).

To verify that the additional decoherence process has indeed ceased after this time, we measure the decays for Carr-Purcell sequences [33] with different numbers of

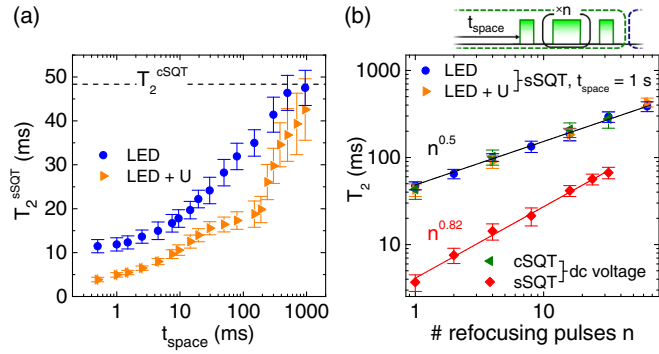


FIG. 2. (a) Coherence times T_2^{sSQT} resulting from the measurements shown in Figs. 1(d) and 1(e). (b) Scaling of T_2 with the number of refocusing pulses n in a Carr-Purcell sequence (dc voltage data reproduced from Ref. [13]). The straight lines are guides to the eye.

refocusing pulses n , as shown in Fig. 2(b). Within error, the observed scaling laws $T_2 \propto n^\beta$ are equal for the satellite SQT for $t_{\text{space}} = 1$ s (LED and LED + U) and the center SQT; the exponent $\beta = 0.5$ indicates a noise spectrum with a $1/f$ frequency dependence [34]. Comparative measurements with a constant voltage applied during the whole pulse sequence (labeled dc voltage, reproduced from Ref. [13]) correspond, in the particular pulse sequence used, to a combined light and bias voltage pulse and a waiting time $t_{\text{space}} = 2$ ms. In agreement with Fig. 2(a), they are strongly influenced by the charge-induced decoherence effects described here, which is also reflected in the different exponent $\beta = 0.82$ for the sSQT. The application of additional voltage pulses during the nuclear echo rf sequence does not have any effect on the coherence times (data not shown), indicating that the influence of field gradients created directly by the contact structures can be neglected in our experiments.

We discuss our model for the charge-induced decoherence of the sSQT with help of Fig. 3, where the electrostatic environment of the As^+ nuclear spin is schematically represented by five defects (circles) and the resulting V_{33} is indicated by the gray contour lines in (b). During the LED or LED + U pulses (i), charges are created in the conduction and valence bands (CB and VB, respectively) and are trapped by the defects [blue and red arrows in Fig. 3(b)(i)]. After the pulses, the charge configuration keeps changing because of interdefect relaxation processes (ii). Therefore, the effective field gradient V_{33} at the position of the As^+ nuclear spin keeps changing, which leads to decoherence mediated by the quadrupole interaction. If the echo sequence is applied during this period, a reduced T_2^{sSQT} is observed. After a longer waiting time, however, the charge configuration becomes stable (iii) and the constant V_{33} does not influence the coherence of the nuclear spin, since its effect is refocused in the echo experiment. Therefore, no additional decoherence

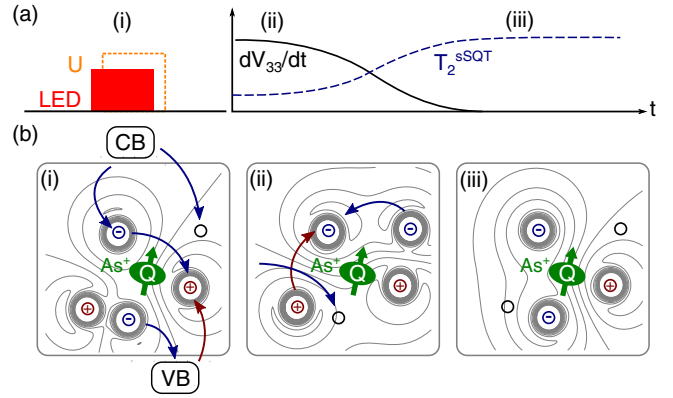


FIG. 3. Timeline (a) and schematic illustration (b) of our model of the charge-induced decoherence process. After the application of light or light-voltage pulses (i), charge recombination leads to fluctuating field gradients [high dV_{33}/dt , (ii)]. Quadrupolar decoherence effects are hence strong, leading to a short T_2^{sSQT} . Once a stable charge environment is reached, this effect vanishes and T_2^{sSQT} is increased (iii). For details, see text.

is generated via the quadrupole interaction and T_2 is equal for the satellite and center SQTs (cf. Fig. 2). Note that the observed time scale of ~ 100 ms is reasonable for recombination processes at low temperatures [35,36].

To study coherences of all orders, we measure the unstrained sample, where the SQTs are degenerate and nonselective rf pulses can be applied. We first consider the density matrix ρ of the nuclear spin ensemble, where the eigenstates are denoted by the diagonal entries and the coherences are given by the off-diagonal entries. Since \mathcal{H} is diagonal, it can be written as $\mathcal{H}^{\text{rot}} = \mathcal{H} + h\nu_{\text{rf}}I_z$ in the rotating frame and the time evolution of the entries ρ_{ij} is given by

$$\rho_{ij}(t) = \rho_{ij}(0)e^{i2\pi\Delta\nu_{ij}t}, \quad (3)$$

where $h\Delta\nu_{ij} = \mathcal{H}_{ii}^{\text{rot}} - \mathcal{H}_{jj}^{\text{rot}}$. In Fig. 4(a), the $\Delta\nu$ are shown in an array plot symbolically representing the density matrix ρ . The orders of the corresponding coherences are indicated by colors; in addition, the transitions that are influenced by first-order quadrupole interaction are shaded in white. Again, the difference between the satellite and center SQTs becomes clear, as the evolution of the former includes ν_Q . The same is true for the DQTs, while the TQT, like the center SQT, is independent of ν_Q . Furthermore, the evolution of each coherence of order p includes the term $p \cdot \Delta\nu_0$, where $\Delta\nu_0 = \nu_0 - \nu_{\text{rf}}$. Note that even in the nominally “unstrained” samples measured in this work, a significant distribution of ν_Q is observed and dominates the linewidth and the dephasing of the relevant transitions [13].

To determine T_2 for the different coherences of the As^+ nuclear spin, we again measure nuclear spin echoes. It is therefore instructive to consider the principle of a spin echo

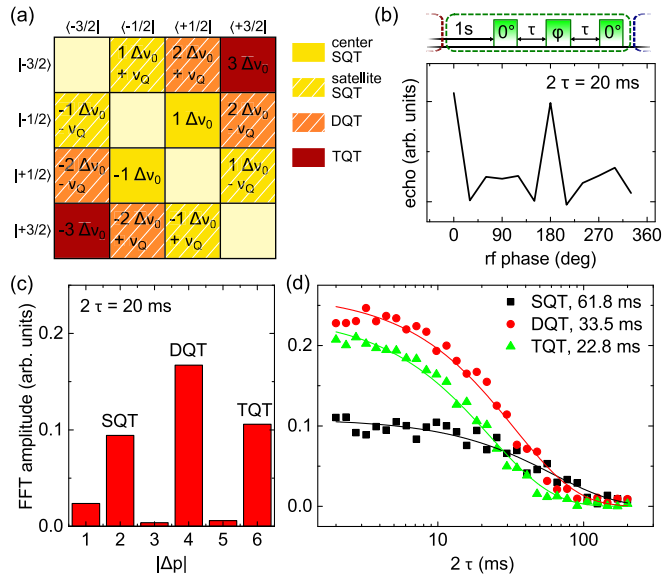


FIG. 4. (a) Summary of the time evolution frequencies $\Delta\nu_{ij}$ of the density matrix elements. (b) Echo amplitude as a function of the phase of the second pulse of the nuclear spin echo sequence. (c) Fourier transform, showing the contributions of different coherence transfer paths to the echo signal. For details see text. (d) Echo decays for the SQT ($\Delta p = \pm 2$), DQT ($\Delta p = \pm 4$), and TQT ($\Delta p = \pm 6$) signals for a waiting time $t_{\text{space}} = 1$ s. The solid lines are fits with exponential functions.

in the density matrix formalism. The first pulse in an echo sequence is used to excite coherences from the initial ground states. They evolve with their respective $\Delta\nu_{ij}$ and during the time τ_1 , each spin collects a phase $\Delta\nu_{ij} \cdot \tau_1$. Then, the second (refocusing) pulse is applied, which transfers the coherence from ρ_{ij} to $\rho_{i'j'}$. It will again evolve, and after the time τ_2 , each spin has collected a total phase of $\Delta\nu_{ij}\tau_1 + \Delta\nu_{i'j'}\tau_2$. Hence, if $\Delta\nu_{ij} = -\Delta\nu_{i'j'}$, the total phase vanishes for $\tau_1 = \tau_2 = \tau$, independently of the actual value of the $\Delta\nu$. Any distribution of $\Delta\nu$ of the ensemble will then refocus, which is the well-known echo effect. Since the propagator is Hermitian, $\Delta\nu_{ij} = -\Delta\nu_{ji}$, and as can be seen with help of Fig. 4(a), the refocusing condition only holds for exactly these pairs. A π pulse, used as a refocusing pulse in the conventional echo sequence, leads to $m_I \rightarrow -m_I$ for all states, which is equivalent to flipping the entries of the density matrix across its center. Comparing the corresponding ν_{ij} , it becomes clear that the refocusing condition is in this case only fulfilled for the center SQT and the TQT, while satellite SQT and DQT are not refocused because of the distribution of the ν_Q . To achieve echoes also from these coherences, we use an echo sequence consisting of three pulses with lengths of 45, 50, and 45 μs , each corresponding to a nutation angle of $\sim 2\pi/3$ [37,38]. Since in such a sequence several different echoes are observed simultaneously, it is necessary to separate the signals corresponding to the refocusing of different coherences. To this end, we use a phase cycle of the phase ϕ of

the refocusing pulse. This adds a shift $\phi\Delta p$ to the phase of the coherence that is transferred from ρ_{ij} to $\rho_{i'j'}$, where $\Delta p = p - p'$ is the difference in coherence order of ρ_{ij} and $\rho_{i'j'}$. Therefore, the detected echo signal will be modified as a function of $\phi\Delta p$ and the different components can be separated by a Fourier transform, equivalent to coherence pathway selection in NMR [27].

We apply the above-mentioned echo sequence after initialization on $m_I = -1/2$. The measured echo amplitude as a function of ϕ is shown as an example in Fig. 4(b); its Fourier transform is given in Fig. 4(c). The largest part of the echo signal is due to a $\Delta p = \pm 4$ coherence transfer (corresponding to the DQT echo); additional components result from $\Delta p = \pm 6$ (TQT echo) and $\Delta p = \pm 2$ (SQT echo). For short τ , significant signals are observed also for $\Delta p = \pm 1$ and ± 3 . Since $\Delta\nu_0$ cannot be refocused in such a coherence path, these contributions vanish with $\tau > T_2^*$ which is ~ 5 ms in our experiments. To measure the different coherence times, we change $\tau = \tau_1 = \tau_2$ and measure the decays of the three coherences. These experiments are performed with a waiting time $t_{\text{space}} = 1$ s to minimize effects of charges created by the light and bias pulses during the readout part of the pulse sequence. The resulting traces are shown in Fig. 4(d) and can be fitted with exponential functions. The extracted coherence times T_2 are 62 ± 10 , 34 ± 5 , and 23 ± 5 ms for SQT, DQT, and TQT, respectively. While we cannot differentiate between the different SQTs, the observed T_2^{SQT} is in agreement with T_2^{cSQT} and T_2^{sSQT} we found in the strained sample above, confirming that quadrupolar decoherence effects are negligible for the chosen t_{space} .

Any decoherence mechanism that can be treated as an effective magnetic field will introduce a fluctuation of $\Delta\nu_0$. Since this is reflected in the time evolution as $p\Delta\nu$, we expect the effect of such disturbances on T_2 to be antiproportional to $|p|$. Accordingly, the ratios $T_2^{\text{SQT}}:T_2^{\text{DQT}}:T_2^{\text{TQT}} = 6:3:2$ should be observed if the limiting process is an effective field interaction. This is in good agreement with experiment, suggesting that a fieldlike interaction, such as the dipolar interaction with environmental ^{29}Si spins [39,40] or fluctuations of the external magnetic field, is responsible for the decay of all coherences in the As^+ nuclear spin system.

In summary, we have characterized coherences of first and higher orders of the nuclear spin of ionized As donors in silicon with and without strain. We have found that, after the application of light or light-voltage pulses, quadrupolar effects can limit the coherence of some transitions and that these influences are minimized when allowing for longer waiting times during the pulse sequence. While it should be noted that the effect is most likely enhanced by the high concentration of irradiation defects in our samples, such decoherence could be relevant in any nuclear spin system with $I > 1/2$. In addition to avoiding electrically active

defects, the decoherence could be reduced by choosing optimal working points in the magnetic field and strain, equivalent to clock transitions with respect to magnetic field [16] or hyperfine interaction [17]. We have also measured echoes connected to higher-order coherences using a phase-cycling technique, exploring the full potential of the four-dimensional Hilbert space. The scaling of the observed coherence times suggest that T_2 in our samples is limited by the interaction with the ^{29}Si nuclear spin bath and the applied technique could be of interest for measurements on donor nuclear spins $I > 1/2$ in isotopically purified ^{28}Si , where this influence is minimized and the limits of the resulting very long coherence times can be investigated. For applications with higher-order quantum systems, usually a more precise control of the higher order coherences will be needed. Pulse shaping and optimal control pulses [41,42] could possibly enable a deterministic excitation of any of the coherences in lightly strained samples and could also allow for a dynamical decoupling for all coherences.

The authors would like to thank Hans-Werner Becker for the implantation, Manabu Otsuka for sample characterization, and Steffen Glaser for fruitful discussion. The work at TUM was supported financially by DFG via SFB 631 and SPP 1601, the work at Keio by KAKENHI (S) No. 26220602 and JSPS Core-to-Core.

* david.franke@wsi.tum.de

- [1] B. E. Kane, *Nature (London)* **393**, 133 (1998).
- [2] L. C. L. Hollenberg, A. S. Dzurak, C. Wellard, A. R. Hamilton, D. J. Reilly, G. J. Milburn, and R. G. Clark, *Phys. Rev. B* **69**, 113301 (2004).
- [3] A. R. Stegner, C. Boehme, H. Huebl, M. Stutzmann, K. Lips, and M. S. Brandt, *Nat. Phys.* **2**, 835 (2006).
- [4] A. Morello, J. J. Pla, F. A. Zwanenburg, K. W. Chan, K. Y. Tan, H. Huebl, M. Möttönen, C. D. Nugroho, C. Yang, J. A. v. Donkelaar, A. D. C. Alves, D. N. Jamieson, C. C. Escott, L. C. L. Hollenberg, R. G. Clark, and A. S. Dzurak, *Nature (London)* **467**, 687 (2010).
- [5] A. M. Tyryshkin, S. Tojo, J. J. L. Morton, H. Riemann, N. V. Abrosimov, P. Becker, H.-J. Pohl, T. Schenkel, M. L. W. Thewalt, K. M. Itoh, and S. A. Lyon, *Nat. Mater.* **11**, 143 (2012).
- [6] M. Steger, K. Saeedi, M. L. W. Thewalt, J. J. L. Morton, H. Riemann, N. V. Abrosimov, P. Becker, and H.-J. Pohl, *Science* **336**, 1280 (2012).
- [7] K. Saeedi, S. Simmons, J. Z. Salvail, P. Dluhy, H. Riemann, N. V. Abrosimov, P. Becker, H.-J. Pohl, J. J. L. Morton, and M. L. W. Thewalt, *Science* **342**, 830 (2013).
- [8] H. Büch, S. Mahapatra, R. Rahman, A. Morello, and M. Y. Simmons, *Nat. Commun.* **4**, 2017 (2013).
- [9] J. J. L. Morton, A. M. Tyryshkin, R. M. Brown, S. Shankar, B. W. Lovett, A. Ardavan, T. Schenkel, E. E. Haller, J. W. Ager, and S. A. Lyon, *Nature (London)* **455**, 1085 (2008).
- [10] J. T. Muhonen, J. P. Dehollain, A. Laucht, F. E. Hudson, R. Kalra, T. Sekiguchi, K. M. Itoh, D. N. Jamieson, J. C. McCallum, A. S. Dzurak, and A. Morello, *Nat. Nanotechnol.* **9**, 986 (2014).
- [11] S. Freer, S. Simmons, A. Laucht, J. T. Muhonen, J. P. Dehollain, R. Kalra, F. A. Mohiyaddin, F. Hudson, K. M. Itoh, J. C. McCallum, D. N. Jamieson, A. S. Dzurak, and A. Morello, [arXiv:1608.07109](https://arxiv.org/abs/1608.07109).
- [12] C. C. Lo, S. Simmons, R. L. Nardo, C. D. Weis, A. M. Tyryshkin, J. Meijer, D. Rogalla, S. A. Lyon, J. Bokor, T. Schenkel, and J. J. L. Morton, *Appl. Phys. Lett.* **104**, 193502 (2014).
- [13] D. P. Franke, F. M. Hrubesch, M. Künzl, H.-W. Becker, K. M. Itoh, M. Stutzmann, F. Hoehne, L. Dreher, and M. S. Brandt, *Phys. Rev. Lett.* **115**, 057601 (2015).
- [14] F. R. Bradbury, A. M. Tyryshkin, G. Sabouret, J. Bokor, T. Schenkel, and S. A. Lyon, *Phys. Rev. Lett.* **97**, 176404 (2006).
- [15] J. Z. Salvail, P. Dluhy, K. J. Morse, M. Szech, K. Saeedi, J. Huber, H. Riemann, N. V. Abrosimov, P. Becker, H.-J. Pohl, and M. L. W. Thewalt, *Phys. Rev. B* **92**, 195203 (2015).
- [16] G. Wolfowicz, A. M. Tyryshkin, R. E. George, H. Riemann, N. V. Abrosimov, P. Becker, H.-J. Pohl, M. L. W. Thewalt, S. A. Lyon, and J. J. L. Morton, *Nat. Nanotechnol.* **8**, 561 (2013).
- [17] P. A. Mortemousque, S. Berger, T. Sekiguchi, C. Culan, R. G. Elliman, and K. M. Itoh, *Phys. Rev. B* **89**, 155202 (2014).
- [18] A. Bienfait, J. J. Pla, Y. Kubo, M. Stern, X. Zhou, C. C. Lo, C. D. Weis, T. Schenkel, M. L. W. Thewalt, D. Vion, D. Esteve, B. Julsgaard, K. Mølmer, J. J. L. Morton, and P. Bertet, *Nat. Nanotechnol.* **11**, 253 (2016).
- [19] T. C. Ralph, K. J. Resch, and A. Gilchrist, *Phys. Rev. A* **75**, 022313 (2007).
- [20] B. P. Lanyon, M. Barbieri, M. P. Almeida, T. Jennewein, T. C. Ralph, K. J. Resch, G. J. Pryde, J. L. O'Brien, A. Gilchrist, and A. G. White, *Nat. Phys.* **5**, 134 (2009).
- [21] N. J. Cerf, M. Bourennane, A. Karlsson, and N. Gisin, *Phys. Rev. Lett.* **88**, 127902 (2002).
- [22] S. D. Bartlett, H. de Guise, and B. C. Sanders, *Phys. Rev. A* **65**, 052316 (2002).
- [23] D. P. Franke, M. P. D. Pflüger, P. A. Mortemousque, K. M. Itoh, and M. S. Brandt, *Phys. Rev. B* **93**, 161303 (2016).
- [24] J. J. Pla, A. Bienfait, G. Pica, J. Mansir, F. A. Mohiyaddin, A. Morello, T. Schenkel, B. W. Lovett, J. J. L. Morton, and P. Bertet, [arXiv:1608.07346](https://arxiv.org/abs/1608.07346).
- [25] P. A. Mortemousque, S. Rosenius, G. Pica, D. P. Franke, T. Sekiguchi, A. Truong, M. P. Vlasenko, L. S. Vlasenko, M. S. Brandt, R. G. Elliman, and K. M. Itoh, *Nanotechnology* **27**, 494001 (2016).
- [26] P. P. Man, in *NMR of Quadrupolar Nuclei in Solid Materials*, edited by R. E. Wasylshen, S. E. Ashbrook, and S. Wimperis (Wiley, Chichester, 2012), p. 3.
- [27] R. R. Ernst, G. Bodenhausen, and A. Wokaun, *Principles of Nuclear Magnetism in One and Two Dimensions* (Oxford University Press, Oxford, England, 1987).
- [28] F. Hoehne, L. Dreher, M. Suckert, D. P. Franke, M. Stutzmann, and M. S. Brandt, *Phys. Rev. B* **88**, 155301 (2013).
- [29] D. P. Franke, F. Hoehne, L. S. Vlasenko, K. M. Itoh, and M. S. Brandt, *Phys. Rev. B* **89**, 195207 (2014).

- [30] D. P. Franke, M. Otsuka, T. Matsuoka, L. S. Vlasenko, M. P. Vlasenko, M. S. Brandt, and K. M. Itoh, *Appl. Phys. Lett.* **105**, 112111 (2014).
- [31] L. Dreher, F. Hoehne, M. Stutzmann, and M. S. Brandt, *Phys. Rev. Lett.* **108**, 027602 (2012).
- [32] F. Hoehne, L. Dreher, D. P. Franke, M. Stutzmann, L. S. Vlasenko, K. M. Itoh, and M. S. Brandt, *Phys. Rev. Lett.* **114**, 117602 (2015).
- [33] H. Y. Carr and E. M. Purcell, *Phys. Rev.* **94**, 630 (1954).
- [34] J. Medford, L. Cywinski, C. Barthel, C. M. Marcus, M. P. Hanson, and A. C. Gossard, *Phys. Rev. Lett.* **108**, 086802 (2012).
- [35] M. Yamaguchi, A. Khan, S. J. Taylor, K. Ando, T. Yamaguchi, S. Matsuda, and T. Aburaya, *J. Appl. Phys.* **86**, 217 (1999).
- [36] P. Dirksen, A. Henstra, and W. T. Wenckebach, *J. Phys.: Condens. Matter* **1**, 7085 (1989).
- [37] I. Solomon, *Phys. Rev.* **110**, 61 (1958).
- [38] H. Abe, H. Yasuoka, and A. Hirai, *J. Phys. Soc. Jpn.* **21**, 77 (1966).
- [39] K. M. Itoh and H. Watanabe, *MRS Commun.* **4**, 143 (2014).
- [40] E. S. Petersen, A. M. Tyryshkin, J. J. L. Morton, E. Abe, S. Tojo, K. M. Itoh, M. L. W. Thewalt, and S. A. Lyon, *Phys. Rev. B* **93**, 161202 (2016).
- [41] T. E. Skinner, T. O. Reiss, B. Luy, N. Khaneja, and S. J. Glaser, *J. Magn. Reson.* **163**, 8 (2003).
- [42] J.-S. Lee, R. R. Regatte, and A. Jerschow, *J. Chem. Phys.* **129**, 224510 (2008).